Electronic Supplementary Material (ESI) for Chemical Communications

Anti-icing surfaces based on enhanced self-propelled jumping of condensed water microdroplets

Qiaolan Zhang,[a,b] Min He,[a] Jing Chen,[a,b] Jianjun Wang,*[a] Yanlin Song*[a] and Lei Jiang[a]

a Beijing National Laboratory for Molecular Sciences (BNLMS), Institute of Chemistry, Chinese Academy of Sciences, Beijing 100190, P. R. China.

b University of Chinese Academy of Sciences, Beijing 100190, P. R. China.

Corresponding E-mail：wangj220@iccas.ac.cn; ylsong@iccas.ac.cn

Preparation of the nanostructured superhydrophobic surface

A thin aluminum film was deposited on a flat silicon substrate via the vacuum deposition with a deposition speed of 1～1.5 Å. Then, the aluminum surface was immersed in a 70^0C water bath for 5 min, and rinsed with water, dried in an oven and modified with 1H, 1H, 2H, 2H-Perfluorodecyltrimethoxysilane (FAS-17) to achieve the superhydrophobicity.

Fabrication of superhydrophobic surfaces with micropore array

Silicon wafer (10 cm. diameter, N type doped with phosphorus, (100) oriented, 525 μm thick) was structured by a standard photolithography technique. Micropores-structured silicon substrates with tunable pore length, pore depths could be fabricated. After the photoresist stripping, the substrates were cleaned by ethanol and acetone. Then they were rendered superhydrophobic via the same process as that of nanostructured superhydrophobic surfaces.

Characterization

The morphologies of surfaces were characterized by a field emission scanning electron microscope (FE-SEM, Hitachi S-4800). The macrodroplets contact angle (CA) on the samples was measured by a CA System (DSA100, Kruss Co. Germ.) at the ambient temperature and the volume of droplets was 4.0 μl. The condensed microdroplets CA on the samples was recorded by the high speed video camera (Phantom, V7.3). An average CA value was obtained by measuring the same sample at least three times. And the adhesion force was measured by a highly sensitive micro electromechanical balance system (Kruss Co. Germ.).

In situ observations of the nucleation, growth and coalescence of condensed microdroplets on structured surfaces

The condensation on structured superhydrophobic surfaces was recorded for 10 min with the speed of 30 frames per seconds (fps) using a high speed imaging system (high-speed video camera, Phantom, V7.3) connected to an optical microscope (Olympus BX51). A humidity controller (Beijing YaDu Technical Company for Cleaning Air, Ltd.) was used to control the relative humidity. The temperature of surfaces was controlled by a linkam heating and cooling stage (Linkam THMS 600). The environmental temperature was about 25 ± 0.8^0C and the relative humidity was about 42.3 ± 2.6 %. The statistic data results from analyzing every frame of recorder videos by free software ImageJ.

Frost formation on various surfaces

The process of ice/frost formation on the normal aluminum surface, the nanostructured superhydrophobic surface and the superhydrophobic surface with 10 μm micropore array were recorded through a high speed imaging system (high-speed video camera, Phantom, V7.3) connected to a 2X objective. When the temperature of the cooling copper stage was lowered to -15^0C, the samples were mounted vertically on the cooling stage. From this point, we recorded the progress of frost formation on various surfaces. The environmental temperature was about 25 ± 0.8^0C and the relative humidity was about 42.3 ± 2.6 %.

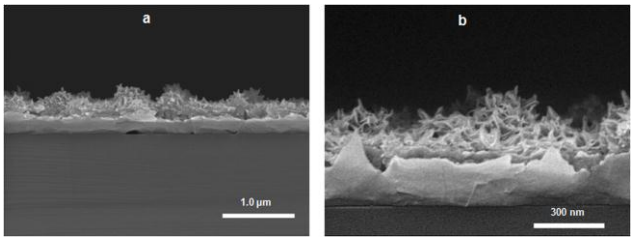

Fig. S1 The side-view (a) and high magnification (b) SEM images of the nanostructured superhydrophobic surface. The diameter and the lengths of nanoclusters was about 300~400 nm and 100~200 nm.

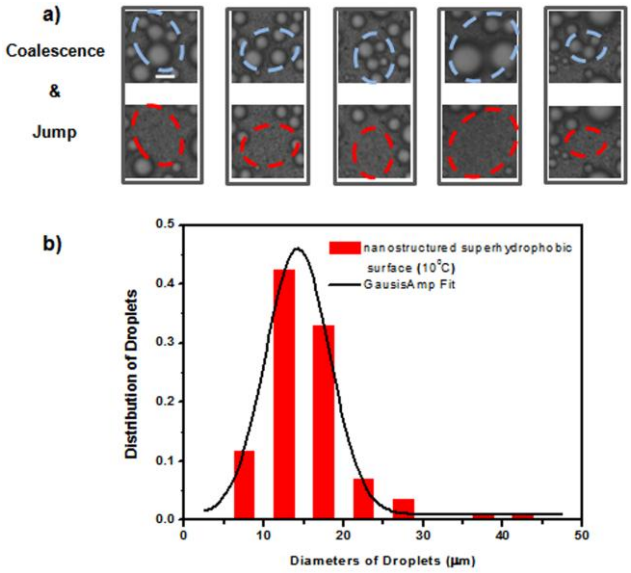

Fig. S2 a) self-propelled jumping on the nanostructured superhydrophobic surface with 10^0C. Light blue dotted circles highlight areas of the surface with droplets just prior to coalescence and subsequent jumping, while red dotted circles highlight areas of the surface right after droplet jumping. The interval was 33.3 ms between sequential images. The scale bar is 20 μm. b) Distribution of the size of condensed water droplets in jumping events and the corresponding GaussAmp fit curves on superhydrophobic surfaces at low supersaturation (1.09, $T_s = 10^0$C). The environmental temperature was 25 ± 0.8^0C and the relative humidity was 42.3 ± 2.6 %.

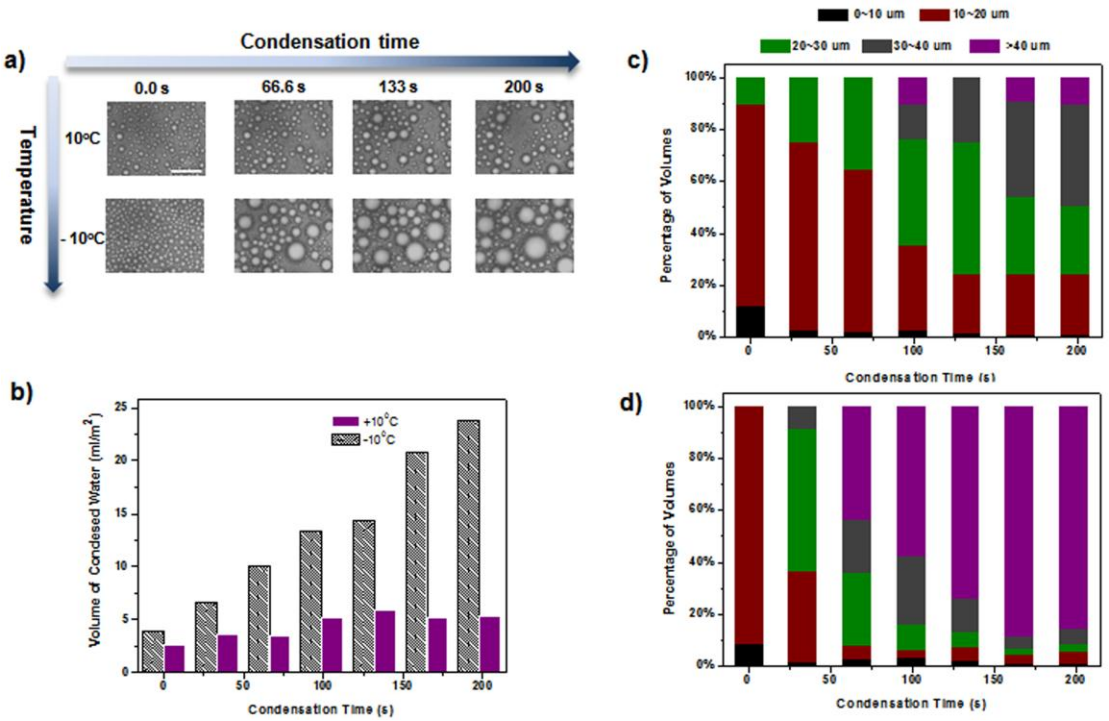

Fig. S3 a) Microscope image sequence of condensation on superhydrophobic surfaces at low supersaturation (1.09, $T_s = 10^0$C) and high supersaturation (4.66, $T_s = -10^o$C). The scale bar is 20 um. b) the volume of condensed water droplets on the whole

surfaces versus time at low supersaturation (1.09, T_s = 10^{0}C) and high supersaturation (4.66, T_s = -10^{o}C). c) and d) show the distribution of volume with various diameters as a function of condensation time on low supersaturation (1.09) and high supersaturation (4.66). The environmental temperature was 25 ± 0.8^{0}C and the relative humidity was 42.3 ± 2.6 %.

A thin aluminum film with a thickness of about 500 nm was deposited on the flat silicon substrate via vacuum deposition. Nanostructured aluminum surfaces were obtained by the reaction of aluminum with hot water, which started with dissolving aluminum and then deposited aluminum hydroxide colloidal particles.[1, 2] It can be seen from scanning electron microscope (SEM) images that the nanostructured aluminum surfaces are covered by hierarchically structured nanostructures, nanoclusters and nanopores (shown in Fig.1b and Fig. S1). The clusters on the nanostructured surface were formed in the vacuum deposition with the speed of 1~1.5 Å/s, and the diameter and the height of nanoclusters were 300~400 nm and 100~200 nm respectively. The outer porous layer is characterized by a convex sub-micrometer cellular structure with sharp rims and a shallow floor, which results in a small liquid solid contact area. The width and depth of cells were about 108 nm and 94.5 nm respectively (Fig. S1). The nanostructures overlay the entire superhydrophobic surfaces with micropore array, i.e., bottom and wall of micropores and space between neighboring micropores, and had not changed the morphologies of micropore array (Fig. S4-A and Fig. 1c).

When the supersaturation was about 1.09 (T_s = 10^{o}C), The self-propelled jumping of condensed microdroplets occurred on the nanostructure superhydrophobic surface. The diameter of most coalescing microdroplets in jumping events was in the range of 10~20 μm (Fig. S2). Increasing the supersaturation to 4.66 (T_s = -10^{o}C), the self-propelled jumping disappeared and the condensed water microdroplets kept on growing with the time (Fig. S3).

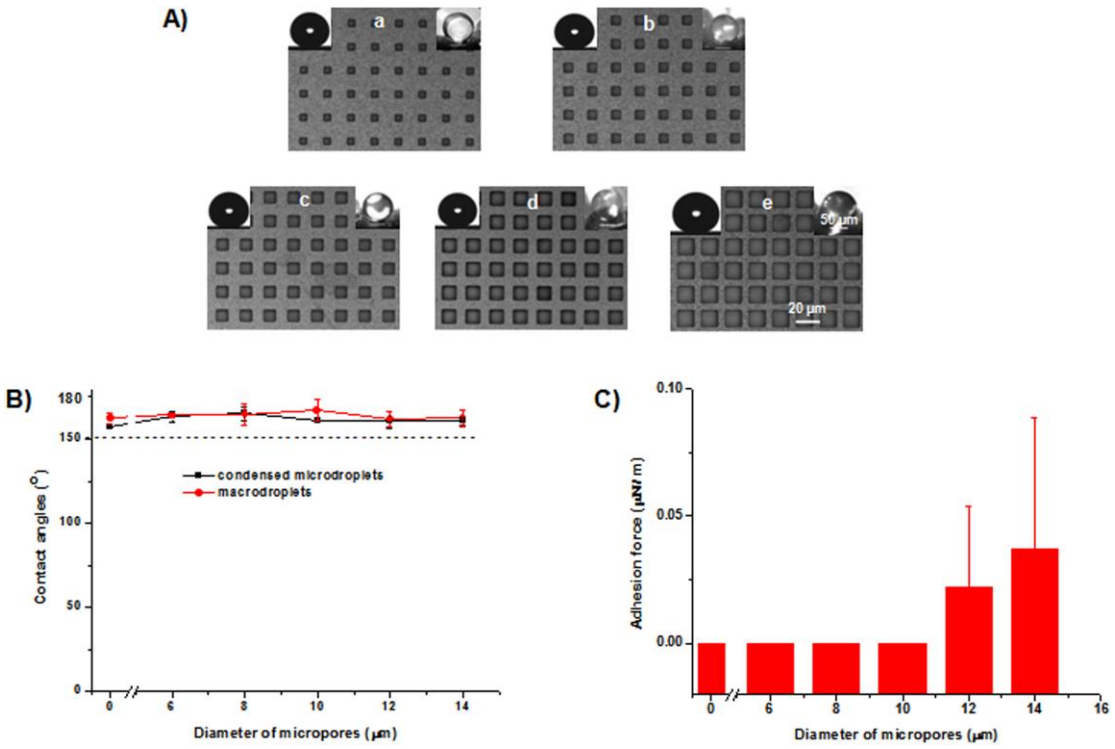

Fig. S4 A) The microscope images of superhydrophobic surfaces with micropore sizes of 6μm (a), 8 μm (b), 10 μm (c), 12 μm (d) and 14 μm (e). The scale bar is 20 μm. Left and right insets of each figure correspond to optical images of macroscopic droplets (4.0 μl) and condensed microdroplets (scale bar is 50 μm) respectively on the corresponding surface. B) The contact angles of macrodroplets (4.0 μl) and condensed microdroplets *versus* the size of micropores of superhydrophobic surfaces with micropore array. All the surfaces were superhydrophobic towards to macrodroplets and condensed microdroplets. C) The adhesion forces on superhydrophobic surfaces with micropore array *versus* the size of micropores. All adhesion forces are less than 0.1μN/m and all surfaces were low-adhesion.

The values of contact angles of macroscopic droplets on nanostructured superhydrophobic surfaces and five superhydrophobic surfaces with a micropore array are almost the same, i.e., around 163 ^{0}, and the values of the contact angles of condensed microdroplets on these six surfaces are almost the same too, i.e., around 161 ^{0} (left insets of Fig. 1b and 1c, insets of Fig S4-A and S4-B). The adhesion forces between a 10 μL macroscopic droplet and various surfaces were low, i.e., less than 0.1 μN/m (Fig. S4-C). All these data show that these surfaces are superhydrophobic to both macroscopic water droplets and condensed microdroplets.

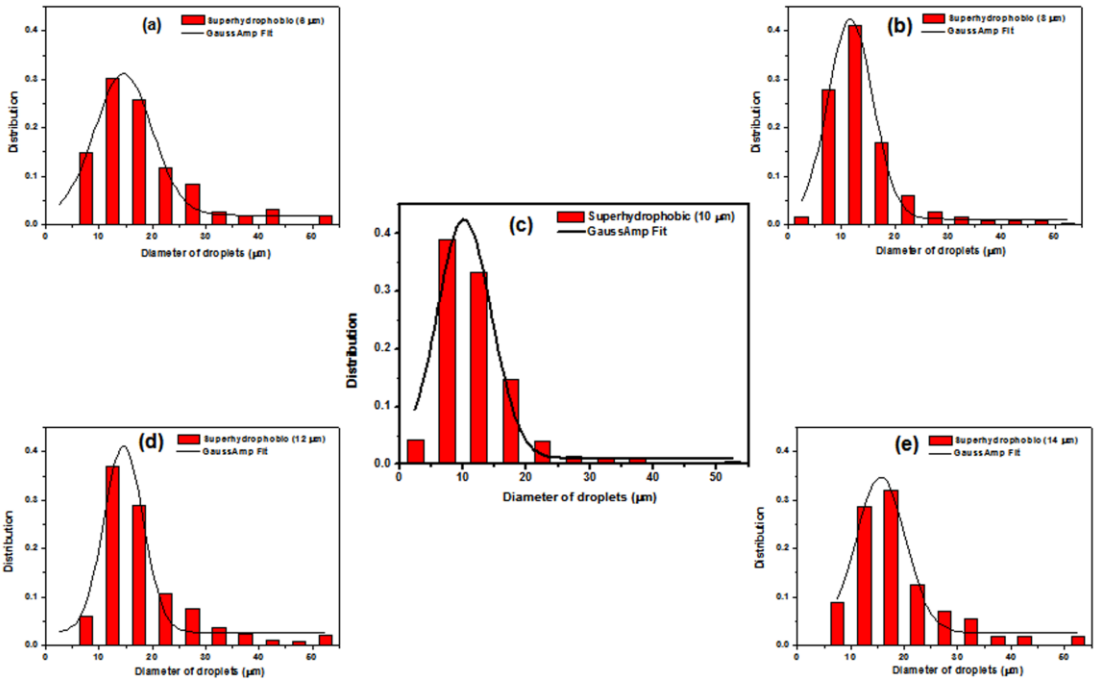

Fig. S5 Distribution of diameters of coalescing microdroplets on superhydrophobic surfaces with micropore array of a) 6 μm, b) 8 μm, c) 10 μm, d) 12 μm and e) 14 μm and the corresponding GaussAmp fit curves at high supersaturation (4.66, T_s = -10^{0}C).. The environmental temperature was 25 ± 0.8^{0}C and the relative humidity was 42.3 ± 2.6 %.

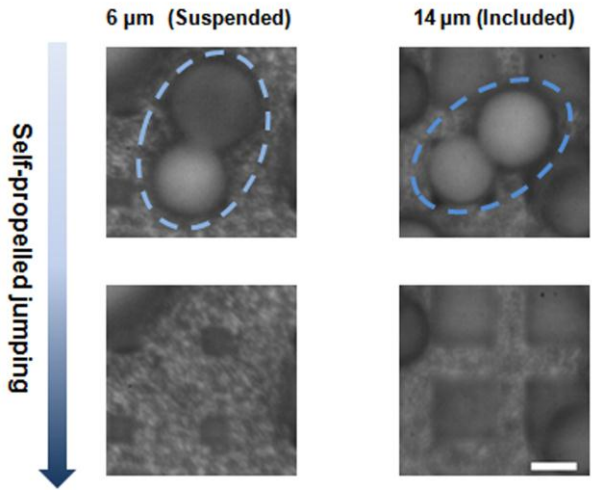

Fig. S6 Typical optical microscopic images of the coalescence of big condensed microdroplets on superhydrophobic surfaces with small micropore (6 μm) and big micropore (14 μm) array at a high supersaturation of 4.66. Light blue dotted circles highlight the microdroplets before coalescence. The interval was 33.3 ms between sequential images. T_s = – 10^{0}C. The environmental temperature was 25 ± 0.8^{0}C and the relative humidity was 42.3 ± 2.6 %. The scale bar is 10μm.

The high jumping frequency and small diameter of coalescing microdroplets in self-propelled jumping endow the fresh nucleation of smaller condensate. Increasing time-averaged density of

small droplet transfers heat more efficiently from the vapor to the surface, which increases the surface temperature and thus retards the ice nucleation.[3-5] In addition, the nucleation of a small droplet on a solid surface is more difficult than a big one and the growth of the interdrop frost front is much slower on the superhydrophobic surface with self-propelled jumping events compared to other surfaces.[6-9] More importantly, the jumping off condensed water microdroplets significantly decrease the total mass of supercooled water on the subfreezing surfaces, that is, the accumulated ice on the surfaces is also reduced remarkably.

In icing experiment, the area of surfaces was 5.3 mm× 5.3 mm. Due to the departing condensed water on the superhydrophobic surface with micropores and the growth of the frost on the normal aluminium surface,[10] the freezing delay was large prolonged and the mass of frost was dramatically decreased as described in the manuscript. Furthermore, this property maintained after tens of icing/deicing cycles. Therefore, the superhydrophobic surface with 10 μm micropore array is an excellent anti-icing surface.

Video 1, 2, 3 and 4 recorded the behavior of condensed microdroplets on the nanostructured superhydrophobic surface, superhydrophobic surfaces with 6μm, 10 μm and 14μm micropore array respectively. The videos are post-processed for upload.

Reference

1. W. Vedder and D. A. Vermilyea, *Trans Faraday Soc*, 1969, **65**, 561-584.
2. M. He, X. Zhou, X. Zeng, D. Cui, Q. Zhang, J. Chen, H. Li, J. Wang, Z. Cao, Y. Song and L. Jiang, *Soft Matter*, 2012, **8**, 2680-2683.
3. X. Chen, J. Wu, R. Ma, M. Hua, N. Koratkar, S. Yao and Z. Wang, *Adv Funct Mater*, 2011, **21**, 4597-4597.
4. C. Dietz, K. Rykaczewski, A. G. Fedorov and Y. Joshi, *Appl Phys Lett*, 2010, **97**, 033104.
5. N. Miljkovic, R. Enright and E. N. Wang, *ACS Nano*, 2012, **6**, 1776-1785.
6. D. Duft and T. Leisner, *Atmos Chem Phys*, 2004, **4**, 1997-2000.
7. D. Ning and X. Y. Liu, *Appl Phys Lett*, 2002, **81**, 445.
8. K. Li, S. Xu, W. Shi, M. He, H. Li, S. Li, X. Zhou, J. Wang and Y. Song, *Langmuir*, 2012, **28**, 10749-10754.
9. J. B. Boreyko and C. P. Collier, ACS Nano, 2013, 7, 1618-1627.
10. B. Na and R. L. Webb, *Int J Heat Mass Tran*, 2004, **47**, 925-936.